Probing function and structure of trehalose-6-phosphate phosphatases from pathogenic organisms suggests distinct molecular groupings

Megan Cross[1], Romain Lepage[1], Siji Rajan[1], Sonja Biberacher[1], Neil D Young[2], Bo-Na Kim[3], Rohan A Davis[1], Mark Coster[1], Robin B Gasser[2], Jeong-Sun Kim[3] & Andreas Hofmann[1,2,4,*]

[1]Eskitis Institute for Drug Discovery, Griffith University, Nathan, Queensland 4111, Australia
[2]Faculty of Veterinary and Agricultural Sciences, The University of Melbourne, Parkville, Victoria 3010, Australia
[3]Department of Chemistry, Chonnam National University, Gwangju 61186, Republic of Korea
[4]Queensland Tropical Health Alliance, Smithfield, Queensland 4878, Australia

[*]Corresponding author: a.hofmann@griffith.edu.au

Journal: *FASEB J.*

This update: 05/10/16

Word count: 4895

Key words: drug targets, enzyme inhibitors, molecular mechanism, structure-function relationships

ABSTRACT: The trehalose biosynthetic pathway is of great interest for the development of novel therapeutics, since trehalose is an essential disaccharide in many pathogens, but neither is required nor synthesised in mammalian hosts. As such, trehalose-6-phosphate phosphatase, a key enzyme in trehalose biosynthesis is likely an attractive target for novel chemotherapeutics. Based on a survey of genomes from a panel of parasitic nematodes and bacterial organisms, and by way of a structure-based amino acid sequence alignment, we derive the topological structure of mono-enzyme trehalose-6-phosphate phosphatases (TPPs) and classify them into three groups. Comparison of the functional roles of amino acid residues located in the active site for TPPs belonging to different groups reveal nuanced variation. Since current literature on this enzyme family shows a tendency to infer functional roles for individual amino acid residues, we investigated the roles of the strictly conserved aspartate tetrad in TPP of the nematode *Brugia malayi* by using a conservative mutation approach. In contrast to aspartate-213, the residue inferred to carry out the nucleophilic attack on the substrate, we found that aspartate-215 and aspartate-428 of *Bm*TPP are involved in the chemistry steps of enzymatic hydrolysis of the substrate. Therefore, we suggest that homology-based inference of functionally important amino acids by sequence comparison for mono-enzyme TPPs should only be carried out for each of the three groups.

Trehalose is an essential disaccharide for many pathogens (including parasites), but is neither required nor synthesised by mammalian cells; the biosynthetic pathway of trehalose thus constitutes a candidate target for chemotherapeutic intervention (1). Of the five different pathways of trehalose synthesis, the only conserved pathway among plants, fungi and invertebrates, was first described for yeast (2). It is regulated by the enzyme trehalose phosphate synthase (TPS) which catalyses the formation of trehalose-6-phosphate from UDP-glucose and glucose-6-phosphate. The phospho group is then removed by trehalose-6-phosphate phosphatase (TPP) to yield trehalose (3, 4). Knockdown of either the TPS genes (*tps-1*, *tps-2*) or the TPP gene (*gob-1*) in the free-living roundworm *Caenorhabditis elegans* showed that an accumulation of the intermediate trehalose-6-phosphate (rather than the absence of trehalose) leads to a lethal phenotype (5). The notable conservation of TPP in pathogenic species and its absence from mammalian hosts makes it an attractive therapeutic target, which stimulated structural and functional characterisation of the enzyme and its family in several species. In fungi, it functions as part of a cooperative multi-enzyme complex with TPS and the two regulatory proteins TPS3 and TSL1 (6–8). In contrast, both TPS and TPP are functional as mono-enzymes in *Escherichia coli*, though the expression of their corresponding genes, *otsA* and *otsB*, from a single operon suggests that their function – and indeed the production of trehalose-6-phosphate – remains tightly regulated (9).

TPP belongs to the superfamily of haloacid dehalogenase (HAD) phosphatases that share a catalytic domain in the topology of a Rossmann fold (reviewed in (10)) which features a magnesium ion surrounded by four conserved aspartate residues. Inserted within the HAD core domain is a so-called cap domain that provides substrate specificity (10). It is generally assumed that the enzymatically active conformation of the enzyme requires the enclosure of the substrate in the active site-interface between the HAD core and the cap domain. This closure involves a rigid-body movement of the cap domain towards the HAD core. This conformational change has not been observed in all TPPs studied thus far, possibly owing to structural differences outside of the conserved HAD motifs between different TPP enzymes, variations in the nature and extent of movement required and the absence of substrate in structures where no closure is observed (10–13). Thus, it is unclear as to whether the formation of a closed conformation is essential for the catalytic function for all TPPs.

The catalytic mechanism (Figure 1) involves a nucleophilic attack by an aspartate in the active site targeting the phosphorus of the phosphate group, which undergoes a conformational change via a trigonal-bipyramidal transition state (14). The release of trehalose renders an enzyme-phosphate conjugate which is hydrolysed in a second step. It is generally believed that a water molecule is

activated by a second aspartate to form a hydroxyl ion which performs a nucleophilic attack on the phosphorus, thus hydrolysing the aspartate-phosphoester and release of the phosphate (10). Based on structures of transition state analogues of hexose phosphate phosphatase of *Bacteroides thetaiotamicron* (15), and, more recently, study of *Cryptococcus neoformans* TPP (12), Asp213 has been inferred to act as the initial nucleophile in the TPP of the parasitic nematode *Brugia malayi* (11). The four conserved aspartate residues in *Bm*TPP are at positions 213, 215, 424 and 428 (Supplemental Figure S1). The investigation of the catalytic site aspartate residues in the latter study was restricted to Asp213 and Asp215 and based on alanine mutations that cannot distinguish the effects of compromised magnesium coordination or inability to attack the phospho-group of the substrate. The same approach was taken in a recent study of TPP from *Mycobacterium tuberculosis* (OtsB2, Rv3372) in which Asp147 (corresponding to Asp213 in *Bm*TPP) was inferred as the initial nucleophile (13).

Importantly, all enzymes of this family investigated thus far possess very high substrate specificity; virtually no enzymatic activity has been observed for any other sugar phospho-ester tested or the commonly used phosphatase substrate *p*-nitropehnylphosphate (1, 16). Moreover, common phosphatase inhibitors do not block TPP activity (1, 16). To date, three crystal structures of mono-enzyme TPPs have been determined, one from each *Thermoplasma acidophilum* (PDB accession code 1u02) (17), *B. malayi* (TPP-like protein; PDB accession code 4ofz) (11) and *M. tuberculosis* (not deposited in the PDB) (13). Additionally, structures of two new fungal TPPs have been solved (12), though it remains unclear whether these function in a complex as seen in other fungal organisms.

Despite the exquisite substrate selectivity of these TPPs and the occurrence of strictly conserved motifs, including four aspartate residues in close vicinity to the catalytically important magnesium ion, there are also significant amino acid sequence variations along the substrate binding surface among different TPPs. These differences appear along the surface contributed by the HAD core domain, but also along the cap domain (Supplemental Figure S1). Owing to such differences the binding pose of trehalose-6-phosphate in different TPPs may not be identical and different conformations are thus potentially possible. Such variations make it difficult to infer interacting residues beyond the strictly conserved catalytic residues from amino acid sequence alignments of TPPs, thus calling for caution when applying the principle of homology.

Here, we surveyed the amino acid sequences of mono-enzyme TPPs from a range of pathogens and evaluated their overall topologies as well as amino acid sequence conservation by means of a structure-based amino acid sequence alignment. For the sequences surveyed, we suggest a classification into three groups of structurally and topologically related TPPs. We also tested the central hypothesis of the currently suggested molecular catalytic mechanism that assumes Asp213 of *Bm*TPP as the initial nucleophile and found that Asp215 and Asp428 showed nucleophilic attack properties. Combined with the structural classification, we suggest that homology-based inference of functionally important amino acids by sequence comparison should be conducted with caution and within each of the three groups.

MATERIALS AND METHODS

Mining of databases for sequences, and secondary structure-based alignment

Amino acid sequences (available in public databases) of putative trehalose-6-phosphate phosphatases from 41 bacterial and parasitic organisms (Supplementary Table S2) were identified by database mining using the BLASTp algorithm (19), the sequence of *Bm*TPP (gb: XM_001893174.1) as well as a keyword search ('trehalose phosphatase'). Secondary structure elements for each amino acid sequence were predicted using the software PSIPRED (20) installed in-house. A secondary structure-based sequence alignment was generated automatically using the software SBAL (21), visually inspected and manually adjusted (see Supplementary Figure S1). Structural and/or functional domains were inferred using all available databases within InterProScan (22) as well as pGenTHREADER (23) installed in-house to survey the PDB.

Protein expression and purification

The codon-optimised expression construct of the TPP gene from *B. malayi* (gb: XM_001893174.1) was obtained from GenScript (USA), ligated into the vector p11 (obtained from The Biodesign Institute, Arizona State University, USA) via *Nde*I and *Bam*HI restriction sites, resulting in a protein construct with an N-terminal fusion peptide ($MGSSH_6SSGRENLYFQGH$). The aspartate mutants *Bm*TPP-D213N, *Bm*TPP-D215N, *Bm*TPP-D424N and *Bm*TPP-D428N were obtained by site-directed mutagenesis.

Expression and purification was performed according to the following general protocol using *E. coli* BL21-AI cells. After transformation of plasmid DNA into *E. coli* and selection on agar plates against ampicillin, a single colony was picked and a liquid overnight culture in 1 l LB^+ medium with 50 $\mu g\ l^{-1}$ ampicillin was grown at 37°C. The overnight culture was used to seed the production culture (8 l) which was grown in seven culture flasks (2 l each) in a shaker incubator at 37°C for ~3.5 h, until the OD_{600} reached ~1.0. Then, the temperature was reduced to 18°C, the culture was induced with 0.2% arabinose, and 15 min later with 0.1 mM IPTG; incubation was continued for 48 h. Cells were harvested by centrifugation for 30 min at 3000 rpm (i.e. an average RCF of 1350×*g*) at 4°C and re-suspended in a buffer containing 100 mM NaCl, 1 mM EDTA, 20 mM TRIS (pH 8.0), 0.1% Triton X-100, 1 mM phenylmethanesulfonyl fluoride, 5 mM benzamidinium chloride. For cell lysis, the suspension was subjected to multiple freeze-thaw cycles and subsequent sonication. The resulting suspension was cleared by high-speed centrifugation (38000×*g*, 30 min, 4°C), and the supernatant was then diluted three-fold with equilibration buffer (20 mM TRIS, pH 8.0) and subjected to anion exchange chromatography with QA52 resin (0-1 M NaCl, 20 mM TRIS, pH 8.0). Fractions containing the appropriate protein (assessed by SDS-PAGE) were combined and loaded onto Ni^{2+}-nitrilotriacetic acid resin (Qiagen, Doncaster, Victoria, Australia) equilibrated with a buffer containing 100 mM NaCl, 20 mM TRIS, pH 8.0. An imidazole step gradient was applied to elute protein fractions that were again assessed by SDS-PAGE and appropriate fractions pooled.

The N-terminal hexa-His-fusion peptide was proteolytically removed from the target proteins using tobacco etch virus (TEV) protease. The TEV protease bacterial expression plasmid was a kind gift by the laboratory of Opher Gileadi (Nuffield Department of Medicine, University of Oxford). The protease (with mutation S219V) was expressed and purified as a self-cleaving N-terminal fusion construct with maltose binding protein, following generic protocols. Purified TEV protease was stored in glycerol-containing aliquots containing ~1 mg protease at -20°C. For proteolytic cleavage of the fusion peptide, the pooled fractions were dialysed overnight against a buffer containing 0.5 mM EDTA, 1 mM DTT, 100 mM NaCl and 20 mM TRIS (pH 8.0). 1 mg of purified His-TEV protease was then added per 50 ml of the dialysed sample and the mixture incubated for 48 h at 4°C. The non-tagged target protein was isolated by loading the reaction mixture onto equilibrated Ni^{2+}-nitrilotriacetic acid resin in the presence of 5 mM imidazole, and capturing the flow-through. A final anion exchange chromatography step using Q-Sepharose (0-1 M NaCl, 20 mM TRIS, pH 8.0) completed the purification. Purified protein samples (see Supplementary Figure S3) were dialysed against a buffer containing 100 mM NaCl, 1 mM $MgCl_2$, 1 mM DTT and 20 mM TRIS (pH 8.0), and concentrated by ultrafiltration using an Amicon Ultra cartridge (Merck, Kilsyth, VIC, Australia) with 30 kDa cutoff. *Bm*TPP wild-type, *Bm*TPP-D215N and *Bm*TPP-D428N were subjected to mass spectrometry to validate their identity by MS fingerprinting (see Supplementary Table S4). CD spectroscopy of purified proteins indicated the presence of the expected secondary structure elements (Supplementary Figure S5).

Synthesis of trehalose-6-phosphate

α,α'-Trehalose-6-monophosphate was synthesised using the published procedure (24) with slight modifications (see Supplementary Materials and Methods).

Enzyme assay

Relative phosphatase activity of wild-type and mutant *Bm*TPP was assessed without removal of the

N-terminal fusion peptides. The purified recombinant proteins were tested at 2.5 μM in a buffer solution comprising of 100 mM NaCl, 20 mM TRIS (pH 7.5) and 200 μM trehalose-6-phosphate. Inhibition by EDTA was tested at a concentration of 10 mM. Reactions were set up in triplicate in a 96-well plate at room temperature and were stopped after 15 min by addition of 100 μl of BIOMOL® Green reagent (Enzo Life Sciences, New York, USA). Absorbance at 620 nm was measured after 15 min using a Biotek plate reader.

Atomic emission spectroscopy

Metal content analysis of bacterially expressed and purified *Bm*TPP proteins ($\rho^* = 1$ mg mL^{-1}) was carried out using inductively coupled plasma atomic emission spectroscopy for magnesium with an Optima 8300 instrument (Perkin Elmer, Glen Waverley, VIC, Australia). Excess magnesium present in storage buffer was removed by desalting of samples with Zeba Spin columns (Thermo Fisher Scientific, Massachusetts, USA). Calibration curves were obtained using serial dilutions of 1000 ppm standards (ICP-AES analytical standards; Perkin Elmer) for these metals.

RESULTS

Appraisal of TPP structural topology among different species of bacteria and nematodes

Frequently, TPP sequences in databases are designated as 'hypothetical proteins' or, erroneously, as 'trehalose 6-phosphate synthase' (which likely occurs due to automated annotation that recognises the conserved HAD core domain). For these reasons, we curated mono-enzyme TPP sequences representing a range of organisms of considerable interest as target pathogens for novel therapeutics.

This survey of genomes of prokaryotic and eukaryotic organisms shows that TPP is a conserved enzyme among the 41 species included here (see Supplementary Figure S1, Supplementary Table S2). Combining the structural information from the *T. acidophilum*, *B. malayi* and *M. tuberculosis* TPP crystal structures with secondary structure prediction of the conceptually translated sequences of TPPs obtained from databases, three different structural topologies could be derived (Figure 2). All nematode TPPs included in this survey adopt the topology of *Bm*TPP, consisting of an N-terminal extension of variable length and an MIT-like domain which is connected to the HAD core domain by a helical linker (11). The cap domain is attached the HAD core domain by two hinge-like loop regions of about 8-10 residues each. In contrast, the other bacterial and archaeal TPPs (with exception of mycobacterial TPPs, but including the protein from *M. smegmatis*) comprise only the HAD core and cap domains. In mycobacteria, the N-terminal domain preceding the HAD core/cap domains forms an αβα fold and shares structural similarity with some hydrolases as well as the mycobacterial response regulator protein mtrA (13).

Enzymatic activity of *Bm*TPP wild-type and mutants

Current knowledge of the TPP molecular catalytic mechanisms is based on structural information about transition state analogues and substrate-bound structures of catalytically inactive enzymes. In particular, Asp25 in the TPP from *Candida albicans* (12) and Asp8 in the HAD phosphatase from *B. thetaiotamicron* (15) were involved in transition state analogues in the crystal structure. Additionally, Asp25 from *Cryptococcus neoformans* was shown to be actively involved in the catalytic reaction mechanism by means of an Asp→Asn mutation. These residues both correspond to Asp213 in *B. malayi.*

Four strictly conserved aspartate residues are found in the direct vicinity of the magnesium ion of TPPs and three of them are involved in coordination of the metal ion. Loss of the magnesium ion has been observed previously to result in strongly reduced catalytic activity (18). In order to probe the involvement of individual aspartate side chains in the enzymatic reaction, it is thus important to retain the capability of the mutant protein to coordinate the metal ion. Thus, we elucidated the phosphohydrolase activity of four mutant *Bm*TPP proteins (Asp213Asn, Asp215Asn, Asp424Asn and Asp428Asn) in comparison to that of the wild-type protein (Figure 3). Although the activity of

Asp213Asn and Asp424Asn was indistinguishable from that of the wild-type protein, Asp215Asn and Asp428Asn showed a significantly reduced phosphohydrolase activity at levels of 24% and 13% of the wild-type, respectively. In the presence of the metal chelator EDTA, all five proteins showed reduced enzymatic activity. In the case of Asp215Asn, the residual activity reduced even further. This indicates that all Asp→Asn mutants were still able to coordinate the magnesium ion. This is further supported by metal analysis of purified *Bm*TPP wild-type and mutant proteins using ICP-AES, which showed that all protein samples possessed the same amounts of magnesium. The fact that the addition of EDTA did not lead to any further significant reduction of the enzymatic activity of Asp428Asn indicates that Asp428 is not required for the coordination of the metal ion, which is in agreement with the crystal structure.

DISCUSSION

Previous mutagenesis studies of *B. malayi* and *M. tuberculosis* TPPs employed alanine mutants to probe various residues in the catalytic and substrate binding site of these proteins (11, 13). For functionally relevant aspartate residues, such an approach does not allow the discrimination between the metal coordination function and a potential involvement in the chemical steps of the catalytic process. Furthermore, a frequently employed methodology for establishment of structure-function relationships is the inference of functional roles of individual amino acids of a protein based on amino acid sequence homology. For TPPs, an argument often found in the literature is the inference of one particular conserved aspartate residue as the attacking nucleophile (11, 13). While this particular residue has been shown to be a nucleophile in three different TPP proteins (*C. neoformans*, *C. albicans* and *B. thetaiotamicron*) (12, 15), there is no conclusive experimental evidence for these enzymes in *B. malayi* and *M. tuberculosis*. Moreover, despite the strict conservation of four aspartate residues in the immediate vicinity of the catalytically important magnesium ion, only three of these residues have been studied experimentally (11, 13).

To address this gap in knowledge, we probed the functional involvement of all four strictly conserved aspartate residues using TPP of the nematode *B. malayi*. In contrast to the current assumptions, Asp213 was not involved in the chemistry steps of the catalytic phosphohydrolase activity. The data obtained with four asparagine mutants showed that mutation of Asp215 and Asp428 led to a substantial impairment of catalytic activity. This finding indicates that in *B. malayi*, Asp215 is most likely the attacking nucleophile that forms a covalent bond with the substrate and Asp428 activates a water molecule that acts as a nucleophile in the second step of the catalytic process. However, in the absence of a three-dimensional structure of either the substrate-bound protein or a transition state analogue, the reverse assignment of roles cannot be excluded.

The survey and structure-based amino acid sequence alignment of mono-enzyme TPP sequences from a variety of pathogenic organisms revealed that TPP enzymes from nematodes, bacteria and archaea can be classified into three groups based on their structural topology (Figure 2). Despite the strict conservation of several motifs among all TPPs, there is considerable variation among different species, including in the residues/conformations found in the HAD core and cap regions that form the substrate binding pocket. As evidenced based on the structure-based alignment (Supplementary Figure S1), these differences are mainly apparent when comparing TPPs from different groups. Thus, it seems appropriate to restrict homology-based inference to members that belong to the same group. Accordingly, one can hypothesise that the functional roles of catalytically active aspartate residues are conserved among all TPP members representing nematodes.

Various findings with TPPs from the different groups serve to emphasise the nuanced variation of mechanisms and general properties. A recent study on *Mtb*TPP (13) highlighted functional roles for Asp331 in the active site which is not a member of the strictly conserved tetrad in the family of mono-enzyme TPPs (Asp147, Asp149, Asp330 and Asp334; see Supplementary Figure S1). Notably, Asp331 is conserved among the bacterial and mycobacterial TPPs, but replaced by a threonine in the nematode group. Furthermore, a comparison of the TPPs from *M. tuberculosis* and *M. smegmatis* revealed that both proteins could be inhibited by the antibiotics diumycin and

moenomycin (1). Interestingly, while *Msm*TPP was inhibited by both antibiotics over the entire dose range tested, the enzymatic activity of *Mtb*TPP was activated up to 100 mg mL^{-1} and only inhibited at concentrations beyond 140 mg mL^{-1} of antibiotic. The different behaviour of *Mtb*TPP and *Msm*TPP in this respect coincides with their separation into two different groups of mono-enzyme TPPs, thus providing further support for the proposed grouping.

CONCLUSIONS

Recently, the family of trehalose-6-phosphate phosphatases has received increased attention and several enzymes from pathogenic organisms have been characterised to varying degrees with respect to crystal structures and enzyme activity. The availability of such information is a requirement for rational and targeted drug discovery. In the context of pathogen-host interactions, the absence of TPP from mammalian hosts and the fact that its knockdown in the free-living nematode *Caenorhabditis elegans* results in a lethal phenotype (5) are key reasons why this protein constitutes an attractive target for therapeutic intervention. In the present study, we clarified the functional roles of strictly conserved residues around the catalytically important magnesium ion in nematode TPP and provided a classification scheme for mono-enzyme TPPs from a range of pathogens.

ACKNOWLEDGMENTS

Mass spectrometric analysis was undertaken at the Australian Proteome Analysis Facility (APAF), the infrastructure provided by the Australian Government through the National Collaborative Research Infrastructure Strategy (NCRIS). We gratefully acknowledge James Cameron (Griffith University) for help with the ICP-AES measurements. Research in the investigators' laboratories is funded by the Australian Research Council, the National Health and Medical Research Council (AH, RBG, NDY), the Rebecca L. Cooper Medical Research Foundation (AH) and Chonnam National University (2015-0597, JSK). The Equity Trustees PhD Scholarship (MC) and the NHMRC Career Development Fellowship (NDY) are gratefully acknowledged.

AUTHOR CONTRIBUTIONS

AH and MC conceived the study; AH, MC, JSK and RBG designed experiments; MC, NDY, AH and RBG performed the database surveys; MC, BNK and SB produced proteins; MC performed enzymatic assays; RL, SR, MC and RAD performed organic synthesis; MC and AH analysed data and wrote the paper with critical input from all authors.

REFERENCES

1. Edavana, V. K., Pastuszak, I., Carroll, J. D., Thampi, P., Abraham, E. C., and Elbein, A. D. (2004) Cloning and expression of the trehalose-phosphate phosphatase of Mycobacterium tuberculosis: comparison to the enzyme from Mycobacterium smegmatis. *Arch. Biochem. Biophys.* **426**, 250–257
2. Cabib, E. and Leloir, L. F. (1958) The biosynthesis of trehalose phosphate. *J. Biol. Chem.* **231**, 259–275
3. Lapp, D., Patterson, B. W., and Elbein, A. D. (1971) Properties of a Trehalose Phosphate Synthetase from Mycobacterium smegmatis ACTIVATION OF THE ENZYME BY POLYNUCLEOTIDES AND OTHER POLYANIONS. *J. Biol. Chem.* **246**, 4567–4579
4. Matula, M., Mitchell, M., and Elbein, A. D. (1971) Partial purification and properties of a highly specific trehalose phosphate phosphatase from Mycobacterium smegmatis. *J. Bacteriol.* **107**, 217–222
5. Kormish, J. D. and McGhee, J. D. (2005) The C. elegans lethal gut-obstructed gob-1 gene is trehalose-6-phosphate phosphatase. *Dev. Biol.* **287**, 35–47
6. Reinders, A., Bürckert, N., Hohmann, S., Thevelein, J. M., Boller, T., Wiemken, A., and De Virgilio, C. (1997) Structural analysis of the subunits of the trehalose-6-phosphate synthase/phosphatase complex in Saccharomyces cerevisiae and their function during heat shock. *Mol. Microbiol.* **24**, 687–695
7. De Virgilio, C., Bürckert, N., Bell, W., Jenö, P., Boller, T., and Wiemken, A. (1993) Disruption of TPS2, the gene encoding the 100-kDa subunit of the trehalose-6-phosphate synthase/phosphatase complex in Saccharomyces cerevisiae, causes accumulation of trehalose-6-phosphate and loss of trehalose-6-phosphate phosphatase activity. *Eur. J. Biochem. FEBS* **212**, 315–323
8. Bell, W., Klaassen, P., Ohnacker, M., Boller, T., Herweijer, M., Schoppink, P., Van der Zee, P., and Wiemken, A. (1992) Characterization of the 56-kDa subunit of yeast trehalose-6-phosphate synthase and cloning of its gene reveal its identity with the product of CIF1, a regulator of carbon catabolite inactivation. *Eur. J. Biochem. FEBS* **209**, 951–959
9. McDougall, J., Kaasen, I., and Strøm, A. R. (1993) A yeast gene for trehalose-6-phosphate synthase and its complementation of an Escherichia coli otsA mutant. *FEMS Microbiol. Lett.* **107**, 25–30
10. Burroughs, A. M., Allen, K. N., Dunaway-Mariano, D., and Aravind, L. (2006) Evolutionary genomics of the HAD superfamily: understanding the structural adaptations and catalytic diversity in a superfamily of phosphoesterases and allied enzymes. *J. Mol. Biol.* **361**, 1003–1034
11. Farelli, J. D., Galvin, B. D., Li, Z., Liu, C., Aono, M., Garland, M., Hallett, O. E., Causey, T. B., Ali-Reynolds, A., Saltzberg, D. J., Carlow, C. K. S., Dunaway-Mariano, D., and Allen, K. N. (2014) Structure of the trehalose-6-phosphate phosphatase from Brugia malayi reveals key design principles for anthelmintic drugs. *PLoS Pathog.* **10**, e1004245
12. Miao, Y., Tenor, J. L., Toffaletti, D. L., Washington, E. J., Liu, J., Shadrick, W. R., Schumacher, M. A., Lee, R. E., Perfect, J. R., and Brennan, R. G. (2016) Structures of trehalose-6-phosphate phosphatase from pathogenic fungi reveal the mechanisms of substrate recognition and catalysis. *Proc. Natl. Acad. Sci. U. S. A.* **113**, 7148–7153
13. Shan, S., Min, H., Liu, T., Jiang, D., and Rao, Z. (2016) Structural insight into dephosphorylation by trehalose 6-phosphate phosphatase (OtsB2) from Mycobacterium tuberculosis. *FASEB J.* **epub ahead of print**
14. Lahiri, S. D., Zhang, G., Dunaway-Mariano, D., and Allen, K. N. (2003) The pentacovalent phosphorus intermediate of a phosphoryl transfer reaction. *Science* **299**, 2067–2071
15. Lu, Z., Dunaway-Mariano, D., and Allen, K. N. (2008) The catalytic scaffold of the haloalkanoic acid dehalogenase enzyme superfamily acts as a mold for the trigonal bipyramidal transition state. *Proc. Natl. Acad. Sci. U. S. A.* **105**, 5687–5692

16. Klutts, S., Pastuszak, I., Edavana, V. K., Thampi, P., Pan, Y.-T., Abraham, E. C., Carroll, J. D., and Elbein, A. D. (2003) Purification, cloning, expression, and properties of mycobacterial trehalose-phosphate phosphatase. *J. Biol. Chem.* **278**, 2093–2100
17. Rao, K. N., Kumaran, D., Seetharaman, J., Bonanno, J. B., Burley, S. K., and Swaminathan, S. (2006) Crystal structure of trehalose-6-phosphate phosphatase-related protein: biochemical and biological implications. *Protein Sci. Publ. Protein Soc.* **15**, 1735–1744
18. Kushwaha, S., Singh, P. K., Rana, A. K., and Misra-Bhattacharya, S. (2011) Cloning, expression, purification and kinetics of trehalose-6-phosphate phosphatase of filarial parasite Brugia malayi. *Acta Trop.* **119**, 151–159
19. Altschul, S. F., Madden, T. L., Schäffer, A. A., Zhang, J., Zhang, Z., Miller, W., and Lipman, D. J. (1997) Gapped BLAST and PSI-BLAST: a new generation of protein database search programs. *Nucleic Acids Res* **25**, 3389–3402
20. Bryson, K., McGuffin, L. J., Marsden, R. L., Ward, J. J., Sodhi, J. S., and Jones, D. T. (2005) Protein structure prediction servers at University College London. *Nucleic Acids Res.* **33**, W36–W38
21. Wang, C. K., Broder, U., Weeratunga, S. K., Gasser, R. B., Loukas, A., and Hofmann, A. (2012) SBAL: a practical tool to generate and edit structure-based amino acid sequence alignments. *Bioinforma. Oxf. Engl.* **28**, 1026–1027
22. Jones, P., Binns, D., Chang, H.-Y., Fraser, M., Li, W., McAnulla, C., McWilliam, H., Maslen, J., Mitchell, A., Nuka, G., Pesseat, S., Quinn, A. F., Sangrador-Vegas, A., Scheremetjew, M., Yong, S.-Y., Lopez, R., and Hunter, S. (2014) InterProScan 5: genome-scale protein function classification. *Bioinforma. Oxf. Engl.* **30**, 1236–1240
23. Lobley, A., Sadowski, M. I., and Jones, D. T. (2009) pGenTHREADER and pDomTHREADER: new methods for improved protein fold recognition and superfamily discrimination. *Bioinforma. Oxf. Engl.* **25**, 1761–1767
24. Rønnow, T. E., Meldal, M., and Bock, K. (1994) Gram-scale synthesis of alpha,alpha-trehalose 6-monophosphate and alpha,alpha-trehalose 6,6’-diphosphate. *Carbohydr. Res.* **260**, 323–328

Figure legends

Figure 1
A likely mechanism of phosphoester hydrolysis catalysed by TPPs. The nucleophilic attack by one of the active site aspartate residues leads to a covalent intermediate. In a second step, a water molecule is activated by another aspartate residue in the active site, and the resulting hydroxyl ion performs a second nucleophilic attack, which leads to the release of inorganic phosphate and trehalose.

Figure 2
Based on the structural topology (see also Supplementary Figure S1), TPPs from nematodes and bacteria can be classified into three major groups. Abbreviations: NXD – N-terminal extension domain; MIT – microtubule interacting and transport; HAD – haloacid dehalogenase; NTD – N-terminal domain.

Figure 3
Phosphohydrolase activity of wild-type at mutant *Bm*TPPs in the absence and presence of EDTA (10 mM). Enzyme activity was measured using an endpoint assay with trehalose-6-phosphate as substrate. The data shown represent the average and standard error of three independent measurements.

Figures

Figure 1

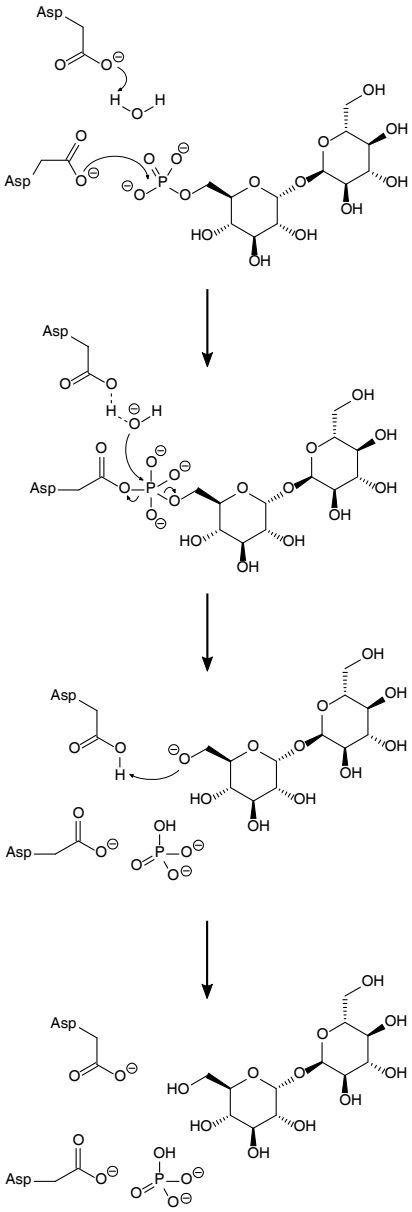

A likely mechanism of phosphoester hydrolysis catalysed by TPPs. The nucleophilic attack by one of the active site aspartate residues leads to a covalent intermediate. In a second step, a water molecule is activated by another aspartate residue in the active site, and the resulting hydroxyl ion performs a second nucleophilic attack, which leads to the release of inorganic phosphate and trehalose.

Figure 2

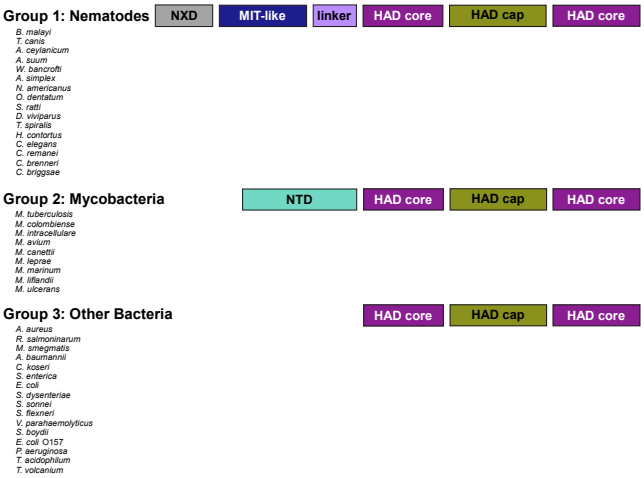

Based on the structural topology (see also Supplementary Figure S1), TPPs from nematodes and bacteria can be classified into three major groups. Abbreviations: NXD – N-terminal extension domain; MIT – microtubule interacting and transport; HAD – haloacid dehalogenase; NTD – N-terminal domain.

Figure 3

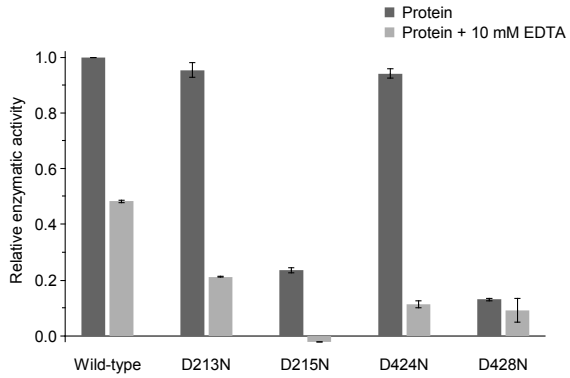

Phosphohydrolase activity of wild-type at mutant *Bm*TPPs in the absence and presence of EDTA. Enzyme activity was measured using an endpoint assay with trehalose-6-phosphate as substrate. The data shown represent the average and standard error of three independent measurements.